Agonist of growth hormone-releasing hormone reduces pneumolysin-induced pulmonary permeability edema

Rudolf Lucas[a,b,1], Supriya Sridhar[a], Ferenc G. Rick[c,d], Boris Gorshkov[a], Nagavedi S. Umapathy[a], Guang Yang[a], Aluya Oseghale[a], Alexander D. Verin[a], Trinad Chakraborty[e], Michael A. Matthay[f], Evgeny A. Zemskov[a], Richard White[b], Norman L. Block[c,d,g], and Andrew V. Schally[c,d,g,1]

[a]Vascular Biology Center and [b]Department of Pharmacology and Toxicology, Georgia Health Sciences University, Augusta, GA 30912; [c]Veterans Affairs Medical Center and South Florida Veterans Affairs Foundation for Research and Education, [d]Department of Pathology, Miller School of Medicine, University of Miami, Miami, FL 33136; [e]Institute for Medical Microbiology, Justus Liebig University Giessen, Giessen, Hessen 35392, Germany; [f]Cardiovascular Research Institute, University of California, San Francisco, CA 94143; and [g]Divisions of Hematology/Oncology and Endocrinology, Department of Medicine, Miller School of Medicine, University of Miami, Miami, FL 33136

Aggressive treatment with antibiotics in patients infected with *Streptococcus pneumoniae* induces release of the bacterial virulence factor pneumolysin (PLY). Days after lungs are sterile, this pore-forming toxin can still induce pulmonary permeability edema in patients, characterized by alveolar/capillary barrier dysfunction and impaired alveolar liquid clearance (ALC). ALC is mainly regulated through Na^+ transport by the apically expressed epithelial sodium channel (ENaC) and the basolaterally expressed Na^+/K^+-ATPase in type II alveolar epithelial cells. Because no standard treatment is currently available to treat permeability edema, the search for novel therapeutic candidates is of high priority. We detected mRNA expression for the active receptor splice variant SV1 of the hypothalamic polypeptide growth hormone-releasing hormone (GHRH), as well as for GHRH itself, in human lung microvascular endothelial cells (HL-MVEC). Therefore, we have evaluated the effect of the GHRH agonist JI-34 on PLY-induced barrier and ALC dysfunction. JI-34 blunts PLY-mediated endothelial hyperpermeability in monolayers of HL-MVEC, in a cAMP-dependent manner, by means of reducing the phosphorylation of myosin light chain and vascular endothelial (VE)-cadherin. In human airway epithelial H441 cells, PLY significantly impairs Na^+ uptake, but JI-34 restores it to basal levels by means of increasing cAMP levels. Intratracheal instillation of PLY into C57BL6 mice causes pulmonary alveolar epithelial and endothelial hyperpermeability as well as edema formation, all of which are blunted by JI-34. These findings point toward a protective role of the GHRH signaling pathway in PLY-induced permeability edema.

pneumonia | cyclic AMP

Severe pneumonia is the leading single cause of mortality worldwide in children less than 5 y old (1). In the US, community-acquired pneumonia affects mainly elderly patients (2). Potent antibiotics and aggressive intensive-care support did not reduce the fatality rate of 20% associated with infections by *Streptococcus pneumoniae*, the main etiological agent of community-acquired pneumonia (1, 2). A major complication of severe pneumonia is pulmonary permeability edema, characterized by dysfunction of the alveolar epithelial/capillary endothelial barrier and impaired alveolar liquid clearance (ALC) (3).

Intriguingly, edema formation can occur days after the initiation of antibiotic therapy, when tissues are sterile and the pneumonia is clearing and correlates with the presence of the bacterial virulence factor pneumolysin (PLY) (4, 5). PLY is a 53-kDa cytoplasmic thiol-activated toxin released during pneumococcal lysis and is implicated in the pathogenesis of pneumococcal disease. This protein has cytolytic and complement-activating properties (4). Lung injury induced by PLY was suggested to result from direct pneumotoxic effects on the alveolar–capillary

barrier rather than from resident or recruited phagocytic cells (6). Cytoplasmic hemolytic PLY is released during autolysis, such as occurs because of antibiotic treatment (7, 8), and subsequently binds to cholesterol in cell membranes, upon which oligomerization and pore formation take place. These pores facilitate increased intracellular Ca^{2+} levels (9), which in turn activate mechanisms leading to contraction of endothelial cells (10, 11). These pathways include both myosin light chain (MLC)-dependent mechanisms and microtubule depolymerization, the latter of which can cause disassembly of adherens junction proteins, such as vascular endothelial (VE)-cadherin (12).

ALC has been shown to inversely correlate with morbidity and mortality in acute lung injury and acute respiratory distress syndrome (ARDS) patients (13). Active Na^+ and Cl^- transport in alveolar type II cells represents the main driving force of net ALC, as demonstrated in the lungs of several different species, including human (14). Na^+ ions in the alveolar lining fluid were shown to passively diffuse into fetal distal lung epithelial and alveolar epithelial type II cells through nonselective cationic channels and Na^+-selective, amiloride-sensitive channels. The most important of these is the epithelial sodium channel (ENaC), located in the apical membrane and consisting of at least three subunits, with the α-subunit of ENaC being crucial for its activity (15, 16). The favorable electrochemical driving force for Na^+ influx is maintained by the basolaterally expressed, ouabain-sensitive Na^+/K^+-ATPase that transports Na^+ into the interstitial space (17).

The hypothalamic peptide growth hormone-releasing hormone (GHRH) stimulates the production and release of growth hormone from pituitary somatotroph cells, after binding to the pituitary GHRH receptor (pGHRH-R) (18, 19). The recent identification of various extrapituitary sources for GHRH production and the demonstration of a direct action of GHRH on several tissues other than the pituitary also indicate that this neuropeptide is a pleiotropic hormone (20). Although peripheral tissues rarely express full-length GHRH-R, splice variants can also be found (21). Thus, GHRH-R and splice variant SV1 are present not only in tumors but also in myocardium, pancreatic β-islet cells, and fibroblasts (22–24). Nonpituitary GHRH can

modulate cell proliferation, especially in malignant tissues (18), promote healing of skin wounds, inhibit cardiomyocyte apoptosis, and reduce infarct size in isolated rat heart after ischemia reperfusion and in vivo after myocardial infarction (21–25). Moreover, GHRH agonists were shown to stimulate cardiac myocytes, to accelerate regeneration of the heart in rats after myocardial infarct, to stimulate pancreatic β-islet cells, and to accelerate wound healing in mice (21–24).

In this study, we demonstrate that human lung microvascular endothelial cells (HL-MVEC), representing important target cells of PLY-induced lung dysfunction (5), express GHRH as well as the splice variants SV1 and SV3 of the GHRH-R. In view of the previously identified cardioprotective effects of GHRH agonists and the current identification of SV1 in HL-MVEC, we have therefore investigated whether the GHRH agonist JI-34 (26) is able to reduce pulmonary permeability edema induced by intratracheal (i.t.) PLY instillation in mice. Our data demonstrate a potent protective activity of this agonist, characterized by a restoration of alveolar Na^+ uptake capacity and a significant improvement of both alveolar epithelial and capillary endothelial barrier function in the lungs.

Results

Expression of GHRH and GHRH-R Splice Variants in HL-MVEC.
Using an RT-PCR approach, we demonstrated the presence of mRNA for GHRH as well as splice variants SV1 and SV3 of pGHRH-R in HL-MVEC (Fig. 1). Interestingly, the presence of mRNA for pGHRH-R could not be detected. Of the detected splice variants, SV1 was shown to be a functional receptor, whereas SV3 is most likely a nonfunctional protein (21). As demonstrated in Table S1 and *SI Results*, the relative expression of SV1 in HL-MVEC was significantly elevated upon treatment with GHRH agonist JI-34. These results prompted us to investigate whether the activation of the functional SV1 receptor in HL-MVEC by means of the potent GHRH agonist JI-34 can interfere with the actions of the pneumococcal virulence factor PLY.

GHRH Agonist JI-34 Blunts Phosphorylation of MLC and VE-Cadherin Induced by PLY as Well as Hyperpermeability in HL-MVEC.
Pathways leading to endothelial cell contraction result in reorganization of the cytoskeletal structures. Phosphorylation of regulatory MLC, catalyzed by either Rho kinase or Ca^{2+}-dependent MLC kinase, leads to actin cytoskeleton rearrangement and to the formation of actin stress fibers, a hallmark of loss of endothelial barrier integrity. Our data demonstrate that PLY treatment (15.5 ng/mL)

leads to a robust MLC phosphorylation within 2 h in HL-MVEC (Fig. 2A) that can be significantly abolished upon a 30-min pretreatment of the cells with JI-34 (1 μM). Adherens junctions (AJ) responsible for barrier integrity in the endothelium can also be disturbed by multiple phosphorylations of VE-cadherin, a major AJ protein (27, 28), which can lead to disassembly of this protein from AJ complexes and disruption of the endothelial cell–cell contacts. In our experiments, we tested the levels of Tyr[658]-phosphorylated VE-cadherin, which are indicative of AJ instability (29). Western blotting data shown in Fig. 2B indicate that PLY treatment (15.5 ng/mL) causes a substantial reduction in total VE-cadherin levels (0.57 of control) but a rise in Tyr[658]-phosphorylated VE-cadherin levels (1.11 of control), as such increasing the ratio of phosphorylated over total VE-cadherin by nearly twofold. Importantly, this PLY-mediated effect is significantly altered by a 30-min pretreatment of the cells with 1 μM JI-34, which leads to a partial restoration of total VE-cadherin levels (0.81 of control) and to a significant reduction of phosphorylated VE-cadherin levels (0.7 of control), thus restoring the phosphorylated over total VE-cadherin ratio to nearly basal levels in HL-MVEC.

JI-34 is able to inhibit both MLC and VE-cadherin phosphorylations, each of which mediates endothelial contraction.
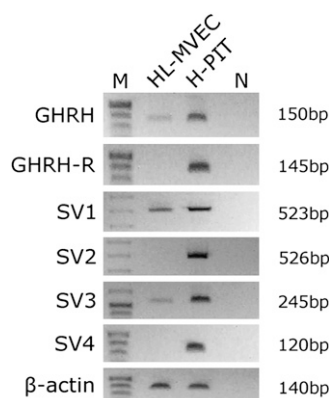

Fig. 2. (A) JI-34 reduces PLY-induced MLC phosphorylation in HL-MVEC. PLY (15.5 ng/mL) increases diphosphorylation of MLC (pp-MLC) within 2 h in HL-MVEC, as assessed by Western blotting. A 30-min pretreatment of the cells with JI-34 (1 μM) significantly reduces this effect. A representative Western blotting experiment (*Upper*) and a data summary of three independent Western blotting experiments (*Lower*; mean ± SD) are shown. (B) Representative VE-cadherin Western blotting experiment in PLY-treated HL-MVEC. PLY (15.5 ng/mL) induces a decrease in total VE-cadherin and an increase in phosphorylated Tyr[658] (pTyr[658]) VE-cadherin, thus increasing the ratio of phosphorylated over total VE-cadherin (1.11:0.57) or β-actin (1.11:0.91) within 2 h of treatment in HL-MVEC. A 30-min pretreatment with JI-34 (1 μM) partially restores total VE-cadherin content and significantly decreases phosphorylated VE-cadherin, thereby normalizing the phosphorylated Tyr[658] VE-cadherin over total VE-cadherin ratio (0.7:0.81).

Fig. 1. RT-PCR analysis of GHRH, GHRH-R, SV1, SV2, SV3, SV4, and β-actin in HL-MVEC and normal human pituitary cells (H-PIT). DNA molecular mass markers are presented in lane M. Human pituitary was used as positive control. Negative controls with no template in real-time PCR are shown in lane N. Product sizes (bp) of corresponding PCR products are shown.
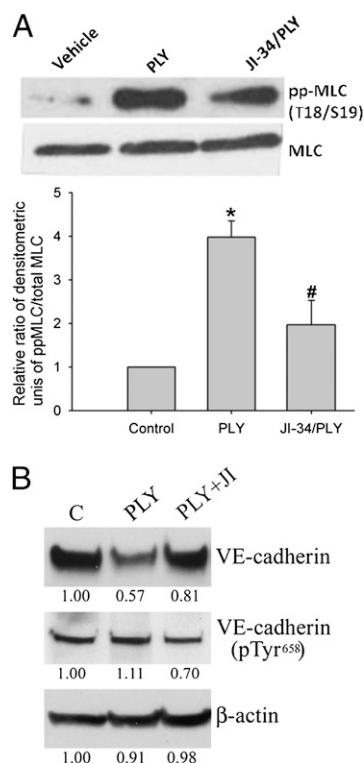
MEDICAL SCIENCES

We therefore investigated the effect of GHRH agonist on PLY-mediated permeability increase in HL-MVEC monolayers by means of assessing transendothelial electrical resistance (TER) by using the electrical cell-substrate impedance sensing (ECIS) system (1600R; Applied Biophysics) or by means of assessing permeability for FITC-dextran. As shown in Fig. 3 A and C, PLY (15.5 ng/mL) induces a rapid and irreversible decrease in TER and significantly increases permeability for FITC-dextran in HL-MVEC monolayers. Pretreatment of the cells for 15 min with 1 µM JI-34 (optimal dose selected by performing dose–response curve in ECIS) conferred a significant protection from PLY-induced hyperpermeability in both assays (Fig. 3 A and C). This dose of JI-34 did not affect basal TER by itself (Fig. 3B). Pre-incubation of the cells for 15 min with 100 µM adenylate cyclase inhibitor SQ22536 before JI-34 application strongly inhibited the agonist's protective effect on PLY-induced hyperpermeability (Fig. 3A), suggesting that JI-34-mediated induction of cAMP generation is crucial for its protective function. We did not find any protection when pretreating the cells with either 1 µM GHRH antagonist MIA-602 (19, 30) or 1 µM bombesin antagonist RC-3940-II. Intriguingly, the GHRH antagonist MIA-602 by itself reduced monolayer resistance at 12 h by ∼30%, whereas RC-3940-II or JI-34 did not affect basal resistance (Fig. 3B), which could indicate that GHRH-R signaling is required for maintaining basal integrity of the microvascular endothelial barrier. Altogether, these results indicate that a GHRH agonist counteracts PLY-induced MLC and VE-cadherin phosphorylation and as such improves barrier function in HL-MVEC.

GHRH Agonist JI-34 Restores Basal Na⁺ Currents in PLY-Treated H441 Cells. Because ALC capacity inversely correlates with morbidity and mortality in patients with acute lung injury and ARDS (13), we also investigated in the human H441 cell line whether PLY can interfere with Na⁺ uptake, which has been shown to be crucial for efficient ALC. Fig. 4A shows a typical current trace of
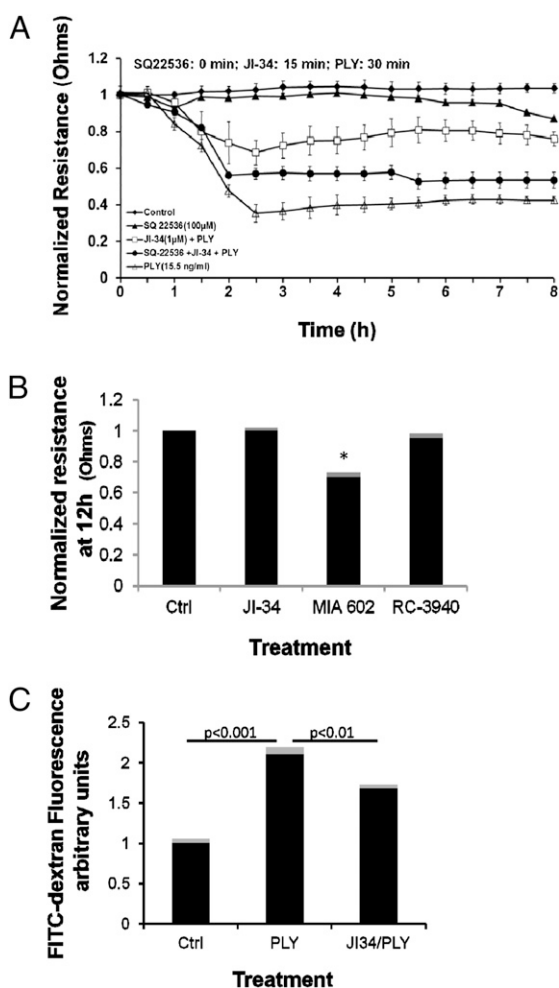

Fig. 3. In vitro permeability measurements in HL-MVEC monolayers. (A) PLY (15.5 ng/mL) induces a rapid decrease in TER, as assessed in ECIS ($n = 8$ per group). A 15-min pretreatment with JI-34 (1 µM) significantly reduces the PLY effect, but this activity is blunted upon a 15-min pretreatment with the adenylate cyclase inhibitor SQ22536 (100 µM). (B) Treatment of HL-MVEC with either GHRH agonist JI-34 alone or with bombesin antagonist RC-3940-II (both at 1 µM) does not affect basal TER after 12 h, whereas the GHRH antagonist MIA-602 (1 µM) significantly reduces TER by ∼30% (mean ± SD; $n = 8$; *$P < 0.05$ vs. control). (C) PLY-induced increase in permeability for FITC-dextran ($n = 4$ per group) and inhibitory effect of JI-34 (1 µM) on this activity in HL-MVEC monolayers measured at 3 h after PLY application.
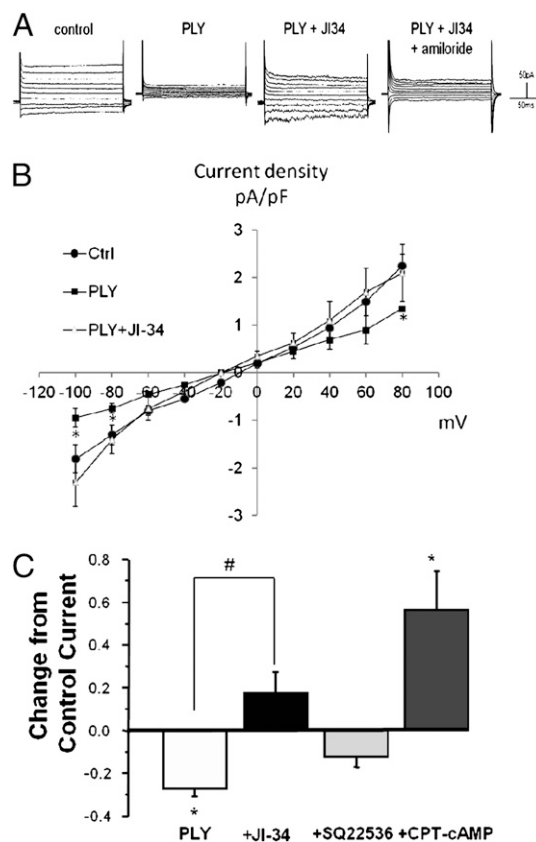

Fig. 4. Assessment of JI-34 effects on Na⁺ uptake capacity in H441 cells. (A) Representative current trace of a single H441 cell recorded in perforated patch–clamp experiments. PLY treatment of H441 cells (30 ng/mL) leads to a significant reduction of both inward and outward currents. The subsequent treatment of the cells with the GHRH agonist JI-34 (1 µM) restores the Na⁺ current, and amiloride (10 µM) significantly blunts this effect. (B) Current density–voltage plot of H441 cell recordings in perforated voltage-gated patch–clamp experiment. PLY treatment significantly reduces inward Na⁺ currents at pulses of −80 and −100 mV. JI-34 treatment restores Na⁺ uptake to nearly basal levels in PLY-treated cells, and amiloride (10 µM) largely blunts its protective effect ($n = 5$; mean ± SD; *$P < 0.05$ vs. PLY group). (C) JI-34 reverses PLY-induced inhibition of inward current in H441 cells via a cAMP-dependent mechanism. Bars represent the average change in steady-state current compared with control (control set to 0.0; $n = 3–8$ cells). *$P < 0.05$ compared with control current; #$P < 0.001$ compared with current in the presence of PLY alone. Drugs were added in cumulative fashion. SQ22536, inhibitor of adenylate cyclase; CPT-cAMP, 8-(4-chlorophenylthio)-cAMP, a membrane-permeable derivative of cAMP.

a recorded H441 cell in which PLY (30 ng/mL) significantly reduces both inward and outward basal Na$^+$ currents and JI-34 is able to restore amiloride-sensitive Na$^+$ uptake. Fig. 4B depicts a current density–voltage plot of five cells per treatment. As demonstrated in Fig. 4C, the Na$^+$ uptake restoration capacity of JI-34 in PLY-treated H441 cells is completely inhibited upon subsequent addition of the adenylate cyclase inhibitor SQ22536 (100 μM). Adding the membrane-permeable cAMP analog 8-(4-chlorophenylthio)-cAMP (50 μM) again increases Na$^+$ uptake significantly. These results thus indicate that PLY reduces amiloride-sensitive Na$^+$-uptake capacity in H441 cells and that JI-34 can restore it to basal levels by activating cAMP generation, which was previously shown to increase amiloride-sensitive Na$^+$ currents in H441 monolayers (31).

JI-34 Protects from PLY-Induced Alveolar–Capillary Barrier Dysfunction in Mice. Our previous results indicated a protective effect of the GHRH agonist JI-34 in PLY-induced endothelial permeability as well as in PLY-mediated Na$^+$ uptake dysfunction, the latter of which causes reduced ALC capacity. Thus, we investigated whether JI-34 can interfere with PLY-induced pulmonary barrier dysfunction in vivo. We assessed alveolar epithelial barrier dysfunction by measuring protein leakage into the bronchoalveolar lavage fluid (BALF) of male C57BL6 mice. Capillary endothelial permeability was evaluated by assessing Evans blue dye-albumin (EBD) incorporation in the lung tissue (n = 10 per group). As shown in Fig. 5A, i.t. instillation of PLY (6.125 μg/kg) induces a significant increase in alveolar epithelial permeability within 24 h. This effect can be efficiently blunted by JI-34 (100 μg/kg), when coapplied i.t. with PLY but not by the bombesin/gastrin-releasing peptide receptor antagonist RC-3940-II (100 μg/kg), which was used as a control peptide. As demonstrated in Fig. 5B, instillation of PLY significantly increased endothelial permeability. This effect was drastically reduced upon cotreatment of the mice with JI-34 but not with RC-3940-II. As demonstrated in Fig. 5C, JI-34 (100 μg/kg) significantly prevented the increase mediated by PLY (6.125 μg/kg) in lung wet-to-dry weight ratio. To investigate whether the protective effect of JI-34 was mainly mediated by its inhibitory effect on direct PLY-mediated barrier dysfunction in the alveolar epithelial and capillary endothelial compartments or rather by an inhibitory effect on inflammatory mediators affecting barrier integrity, we also evaluated its influence on pro- and anti-inflammatory mediator generation, measured in the BALF of the treated animals (n = 6 per group). Our data, presented in Table S2, demonstrate that JI-34 does not interfere with the generation of proinflammatory cytokines or growth factors reported to directly affect pulmonary barrier function, such as TNF, IL-1β, IL-6, and VEGF, but it does change the chemokine response in PLY-treated mice, indicating that it has the potential to modulate specific immune responses. As such, we conclude that JI-34 effects on PLY-mediated endothelial hyperpermeability are mainly mediated by its capacity to induce the barrier-protective second messenger cAMP, which protects from the direct effects of PLY on the pulmonary endothelial monolayer.

Discussion

Although bioactive, mature human GHRH consists of 40–44 aa, the shortest sequence of the hormone that possesses full biological activity consists of only 29 N-terminal residues. This GHRH sequence thus constitutes the core peptide for the development of agonists of GHRH, such as JI-34 (26), or its antagonists. GHRH is expressed in a variety of normal peripheral tissues, uterus, ovary, testis, placenta, cerebral cortex, pituitary, kidney, prostate, liver, and lung. However, the physiological significance of this ectopic production of GHRH has not yet been clarified (20). In this study, we show that the GHRH agonist JI-34 (26) significantly protects HL-MVEC, expressing both GHRH
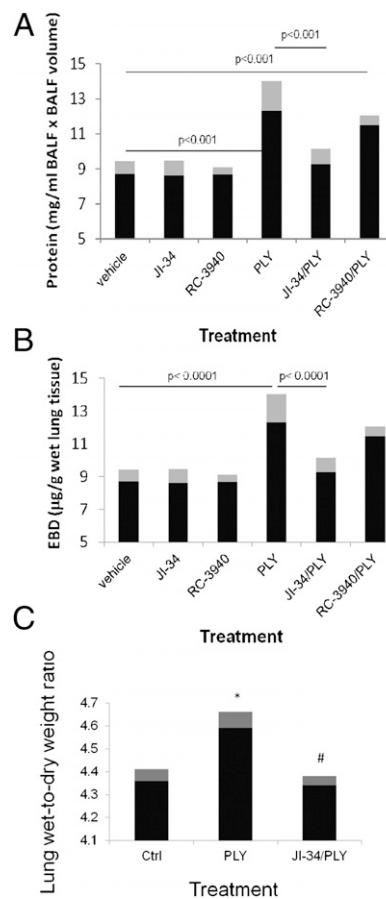

Fig. 5. Assessment of alveolar epithelial and capillary leak as well as edema formation in C57BL6 mice. (A and B) Alveolar epithelial leak assessed by measuring protein content in the BALF (A) and capillary endothelial permeability assessed as EBD incorporation in lung tissue (B) of male C57BL6 mice treated i.t. with PLY (6.125 μg/kg) for 24 h, in the presence or absence of JI-34 and RC-3940-II (both at 100 μg/kg i.t.; n = 10 per group; mean ± SD). (C) JI-34 (100 μg/kg) completely inhibits the increase in lung wet-to-dry weight ratio caused by i.t. PLY instillation (6.125 μg/kg) in male C57BL6 mice (n = 5 per group; mean ± SD; *P < 0.03 vs. control; #P < 0.02 vs. PLY).

and its splice variant receptors SV1 and SV3, from hyperpermeability induced by PLY. Our data indicate that this effect occurs at least in part by reducing PLY-mediated MLC phosphorylation and VE-cadherin loss, two events contributing to endothelial barrier dysfunction.

Binding of ligand to the GHRH-R changes the receptor conformation and activates the G$_s$ α-subunit of the closely associated heterotrimeric G protein on the intracellular side. In the absence of the pituitary type of the GHRH-R, as is the case in human lung endothelial cells, the GHRH-R functions can be performed by the functional SV1 splice variant, which is able to bind GHRH agonists (20). Binding of these agonists to the SV1 splice variant results in stimulation of membrane-bound adenylate cyclase and increased intracellular cAMP generation (20). Subsequently, cAMP can activate protein kinase A (PKA), leading to phosphorylation of the transcription factor cAMP response element-binding protein (CREB). CREB in turn induces the transcription of the pituitary-specific transcription factor Pit-1 gene, which induces the transcription of both growth hormone receptors and GHRH-R (18).

It has been demonstrated that cAMP-mediated activation of PKA, which occurs upon binding of JI-34 to the pGHRH-R or to SV1, attenuates both epithelial and endothelial barrier dysfunction

(32, 33). Moreover, PKA activation in endothelial cells can result in inhibition of Rho kinase by direct phosphorylation of Rho GDP-dissociation inhibitor (RhoGDI), thus preventing the release of the barrier-disruptive RhoA from the RhoA–RhoGDI complex (34). Besides, cAMP potentiates VE-cadherin-mediated cell–cell contacts, thus enhancing endothelial barrier function (32, 33). Phosphorylation of VE-cadherin at Tyr[658] leads to dissociation of this major AJ protein from p120-catenin, which serves as a factor that stabilizes AJ and prevents VE-cadherin endocytosis (28, 29). Therefore, Tyr[658] phosphorylation of VE-cadherin and formation of stress fibers upon MLC phosphorylation provide a basis for rapid endocytosis and degradation of VE-cadherin and cell–cell contact loss. The inhibitory activity of the GHRH agonist JI-34 on PLY-mediated VE-cadherin loss can thus in part be explained by its capacity to activate the cAMP/PKA pathway, by binding to the SV1 receptor, expressed in HL-MVEC. Indeed, pretreatment of the cells with the adenylate cyclase inhibitor SQ22536 completely blunted the barrier-protective activity of JI-34. In this context, it is interesting to note that we could demonstrate that activation of the cAMP/PKA pathway by extracellular β-nicotinamide adenine dinucleotide (β-NAD) protects from PLY-induced endothelial barrier dysfunction (35).

Our findings also indicate that JI-34 is able to restore Na$^+$ uptake, crucial for ALC (3), which we found to be significantly reduced in PLY-treated H441 cells. Our observation that the pore-forming toxin PLY reduces rather than increases Na$^+$ conductance is surprising. However, H441 cells are much less sensitive to permeability increases induced by PLY than HL-MVEC. The capacity of the toxin to activate conventional PKC isoforms that were shown to be able to reduce ENaC expression (36) is most likely responsible for its induction of Na$^+$ uptake dysfunction. In this context, it is interesting to note that activation of PKA mediated by cAMP leads to increased expression of the crucial α-subunit of the ENaC (37), which is the main regulator of apical sodium uptake in type II alveolar epithelial cells. Moreover, cAMP-dependent stimulation of Na$^+$ influx across H441 cells or type II alveolar epithelial cell confluent monolayers was shown to result from activation of an amiloride-sensitive apical Na$^+$ conductance (38).

In conclusion, our results indicate that GHRH-R signaling confers protection against barrier dysfunction induced by PLY in the lungs and can moreover restore impaired Na$^+$ uptake in H441 cells mediated by PLY. Thus, agonists of GHRH should be further investigated as potential therapeutic agents for lung dysfunction in patients with acute lung injury, ARDS, or severe pneumonia in which permeability edema represents a major complication.

Materials and Methods

Whole-Cell Patch–Clamp Recording. Whole-cell currents were measured from metabolically intact H441 cells by using the perforated-patch technique. In contrast to standard whole-cell techniques, perforated-patch recordings provide accurate current measurement with only minimal current decay or loss of soluble cytoplasmic components because of cellular dialysis. Furthermore, endogenous calcium buffering is not inactivated by dialyzing cells with calcium chelators, as required during whole-cell recordings. Thus, the perforated-patch technique provides a more accurate means of measuring whole-cell currents.

H441 cells were grown on 12-mm coverslips and placed in a recording solution containing 140 mM Na acetate, 5 mM KOH, 2 mM MgSO$_4$, 10 mM Hepes, and 10 mM glucose (pH 7.2). Both calcium and chloride were reduced in this solution to attenuate currents resulting from flux of these ions. Patch pipettes with a resistance of 3 MΩ or less were fabricated from capillary tubes using a P-2000 laser pipette puller (Sutter Instrument). To help isolate Na$^+$ currents, the tip of the patch pipette was filled with a solution containing 130 mM Cs$_2$SO$_4$, 5mM CsOH, 2mM CaCl$_2$, 2mM MgCl$_2$, and 10 mM Hepes (pH 7.2). Cs diffuses through the membrane perforations and blocks K channels from the cytoplasmic surface of the membrane. The remainder of the pipette was backfilled with a similar solution to which 200 μg/mL amphotericin B (diluted by sonication from a 50 mg/mL stock in DMSO) was added. Cells were studied only if the voltage drop across the series resistance was reduced to <5 mV within 10–20 min after forming a GΩ seal. Voltage–clamp and voltage pulse generation were controlled with an Axopatch 200B patch–clamp amplifier (Axon Instruments), and data were analyzed with pCLAMP 10.0 (Axon Instruments). Currents were filtered at 2 kHz and digitized at 10 kHz. All substances were diluted into fresh bath solution and perfused into a 1.0-mL recording chamber (Warner Instruments).

Instillation i.t. and Vascular Leakage Assessment in Vivo. Mice were anesthetized with i.p. ketamine (150 mg/kg) and acetylpromazine (15 mg/kg). Then the trachea was exposed. PLY (6.125 μg/kg in saline) was instilled i.t. for 24 h in anesthetized mice via a 20-gauge catheter, with or without JI-34 (100 μg/kg) or RC-3940-II (100 μg/kg). An Evans Blue dye/Albumin mixture (30 mg/kg in saline) was injected into the tail vein 2 h before mice were killed, in order to assess vascular leak (39). Lungs free of blood were weighed and snap-frozen in liquid nitrogen. The left lung was homogenized, incubated with formamide (18 h at +60 °C), and centrifuged at 5,000 × g for 30 min. The optical density of the supernatant was determined spectrophotometrically at 620–750 nm. Extravasated EBD concentration in the lungs was calculated by using a standard curve (microgram of EBD per gram of wet lung tissue), as described previously (39). For quantification of protein or proinflammatory mediators in BALF, collected BALF was centrifuged (500 × g for 15 min at 4 °C), supernatant was centrifuged again (5,000 × g for 15 min at 4 °C), and pure BALF was used to measure total protein with the BCA Protein Assay Kit (Pierce). Absorbance was measured at 540 nm, and protein concentration was determined by using standard curves. Alternatively, cytokine/chemokine/growth factor concentrations were quantified with the multiplex MCYTOMAG-70K assay (EMD Millipore), according to the manufacturer's instructions. Lung wet-to-dry ratios were determined upon weighing lungs immediately after isolation as well as upon drying them for 48 h at 65 °C in an oven. All animal studies conformed to National Institutes of Health guidelines. The experimental procedure was approved by the Georgia Health Sciences University Institutional Animal Care and Use Committee.

For details of cells, mice, biochemicals, PLY purification, peptide analogs preparation, RT-PCR, in vitro TER measurement, in vitro vascular permeability assays, Western blotting analysis, and statistics, refer to the *SI Materials and Methods*.

1. Rudan I, Boschi-Pinto C, Biloglav Z, Mulholland K, Campbell H (2008) Epidemiology and etiology of childhood pneumonia. *Bull World Health Organ* 86:408–416.
2. Waterer GW, Rello J, Wunderink RG (2011) Management of community-acquired pneumonia in adults. *Am J Respir Crit Care Med* 183(2):157–164.
3. Berthiaume Y, Matthay MA (2007) Alveolar edema fluid clearance and acute lung injury. *Respir Physiol Neurobiol* 159:350–359.
4. Rubins JB, et al. (1996) Distinct roles for pneumolysin's cytotoxic and complement activities in the pathogenesis of pneumococcal pneumonia. *Am J Respir Crit Care Med* 153:1339–1346.
5. Witzenrath M, et al. (2006) Role of pneumolysin for the development of acute lung injury in pneumococcal pneumonia. *Crit Care Med* 34:1947–1954.
6. Maus UA, et al. (2004) Pneumolysin-induced lung injury is independent of leukocyte trafficking into the alveolar space. *J Immunol* 173:1307–1312.

7. Anderson R, et al. (2007) Comparison of the effects of macrolides, amoxicillin, ceftriaxone, doxycycline, tobramycin and fluoroquinolones, on the production of pneumolysin by *Streptococcus pneumoniae* in vitro. *J Antimicrob Chemother* 60:1155–1158.
8. Fukuda Y, et al. (2006) Effects of macrolides on pneumolysin of macrolide-resistant *Streptococcus pneumoniae*. *Eur Respir J* 27:1020–1025.
9. Stringaris AK, et al. (2002) Neurotoxicity of pneumolysin, a major pneumococcal virulence factor, involves calcium influx and depends on activation of p38 mitogen-activated protein kinase. *Neurobiol Dis* 11:355–368.
10. Sandoval R, et al. (2001) Ca^{2+} signalling and PKCα activate increased endothelial permeability by disassembly of VE-cadherin junctions. *J Physiol* 533:433–445.
11. Xiong C, et al. (2010) The lectin-like domain of TNF protects from listeriolysin–induced hyperpermeability in human pulmonary microvascular endothelial cells—A crucial role for protein kinase C-α inhibition. *Vascul Pharmacol* 52(5-6):207–213.

12. Petrache I, Birukova A, Ramirez SI, Garcia JG, Verin AD (2003) The role of the microtubules in tumor necrosis factor-α–induced endothelial cell permeability. *Am J Respir Cell Mol Biol* 28:574–581.

13. Ware LB, Matthay MA (2001) Alveolar fluid clearance is impaired in the majority of patients with acute lung injury and the acute respiratory distress syndrome. *Am J Respir Crit Care Med* 163:1376–1383.

14. Matthay MA, Robriquet L, Fang X (2005) Alveolar epithelium: Role in lung fluid balance and acute lung injury. *Proc Am Thorac Soc* 2(3):206–213.

15. Canessa CM, et al. (1994) Amiloride-sensitive epithelial Na⁺ channel is made of three homologous subunits. *Nature* 367:463–467.

16. Eaton DC, Malik B, Bao HF, Yu L, Jain L (2010) Regulation of epithelial sodium channel trafficking by ubiquitination. *Proc Am Thorac Soc* 7(1):54–64.

17. Vadász I, Raviv S, Sznajder JI (2007) Alveolar epithelium and Na,K-ATPase in acute lung injury. *Intensive Care Med* 33:1243–1251.

18. Mayo KE, Godfrey PA, Suhr ST, Kulik DJ, Rahal JO (1995) Growth hormone-releasing hormone: Synthesis and signaling. *Recent Prog Horm Res* 50:35–73.

19. Schally AV, Varga JL, Engel JB (2008) Antagonists of growth-hormone-releasing hormone: An emerging new therapy for cancer. *Nat Clin Pract Endocrinol Metab* 4(1):33–43.

20. Kiaris H, Chatzistamou I, Papavassiliou AG, Schally AV (2011) Growth hormone-releasing hormone: Not only a neurohormone. *Trends Endocrinol Metab* 22:311–317.

21. Rekasi Z, Czompoly T, Schally AV, Halmos G (2000) Isolation and sequencing of cDNAs for splice variants of growth hormone-releasing hormone receptors from human cancers. *Proc Natl Acad Sci USA* 97:10561–10566.

22. Kanashiro-Takeuchi RM, et al. (2010) Cardioprotective effects of growth hormone-releasing hormone agonist after myocardial infarction. *Proc Natl Acad Sci USA* 107:2604–2609.

23. Ludwig B, et al. (2010) Agonist of growth hormone-releasing hormone as a potential effector for survival and proliferation of pancreatic islets. *Proc Natl Acad Sci USA* 107:12623–12628.

24. Dioufa N, et al. (2010) Acceleration of wound healing by growth hormone-releasing hormone and its agonists. *Proc Natl Acad Sci USA* 107:18611–18615.

25. Granata R, et al. (2009) Growth hormone-releasing hormone promotes survival of cardiac myocytes in vitro and protects against ischaemia-reperfusion injury in rat heart. *Cardiovasc Res* 83:303–312.

26. Izdebski J, et al. (1995) Synthesis and biological evaluation of superactive agonists of growth hormone-releasing hormone. *Proc Natl Acad Sci USA* 92:4872–4876.

27. Andriopoulou P, Navarro P, Zanetti A, Lampugnani MG, Dejana E (1999) Histamine induces tyrosine phosphorylation of endothelial cell-to-cell adherens junctions. *Arterioscler Thromb Vasc Biol* 19:2286–2297.

28. Dejana E, Orsenigo F, Lampugnani MG (2008) The role of adherens junctions and VE-cadherin in the control of vascular permeability. *J Cell Sci* 121:2115–2122.

29. Hatanaka K, Simons M, Murakami M (2011) Phosphorylation of VE-cadherin controls endothelial phenotypes via p120-catenin coupling and Rac1 activation. *Am J Physiol Heart Circ Physiol* 300:H162–H172.

30. Pozsgai E, et al. (2011) The effect of a novel antagonist of growth hormone releasing hormone on cell proliferation and on the key cell signaling pathways in nine different breast cancer cell lines. *Int J Oncol* 39:1025–1032.

31. Lazrak A, Matalon S (2003) cAMP-induced changes of apical membrane potentials of confluent H441 monolayers. *Am J Physiol Lung Cell Mol Physiol* 285:L443–L450.

32. Lawrence DW, Comerford KM, Colgan SP (2002) Role of VASP in reestablishment of epithelial tight junction assembly after Ca²⁺ switch. *Am J Physiol Cell Physiol* 282:C1235–C1245.

33. Fukuhara S, et al. (2005) Cyclic AMP potentiates vascular endothelial cadherin-mediated cell-cell contact to enhance endothelial barrier function through an Epac-Rap1 signaling pathway. *Mol Cell Biol* 25(1):136–146.

34. Qiao J, et al. (2008) Phosphorylation of GTP dissociation inhibitor by PKA negatively regulates RhoA. *Am J Physiol Cell Physiol* 295:C1161–C1168.

35. Umapathy NS, et al. (2010) Extracellular β-nicotinamide adenine dinucleotide (β-NAD) promotes the endothelial cell barrier integrity via PKA- and EPAC1/Rac1-dependent actin cytoskeleton rearrangement. *J Cell Physiol* 223(1):215–223.

36. Chen XJ, et al. (2004) Influenza virus inhibits ENaC and lung fluid clearance. *Am J Physiol Lung Cell Mol Physiol* 287:L366–L373.

37. Mustafa SB, et al. (2008) Protein kinase A and mitogen-activated protein kinase pathways mediate cAMP induction of α-epithelial Na⁺ channels (α-ENaC). *J Cell Physiol* 215(1):101–110.

38. Fang X, Song Y, Zemans R, Hirsch J, Matthay MA (2004) Fluid transport across cultured rat alveolar epithelial cells: A novel in vitro system. *Am J Physiol Lung Cell Mol Physiol* 287:L104–L110.

39. Moitra J, Sammani S, Garcia JG (2007) Re-evaluation of Evans Blue dye as a marker of albumin clearance in murine models of acute lung injury. *Transl Res* 150(4):253–265.

MEDICAL SCIENCES